Supplementary Information (SI) for Inorganic Chemistry Frontiers.

Supporting Information

Carbon-Nanotube Wall Nanoengineering Strategy to Stabilize FeNi Nanoparticles and Fe Single Atoms for Rechargeable Zn-Air Batteries

Yi-Yin Yang[1], Lin He[1], Peng-Fei Xie[1], Peng Dong[2], Hao Quan[2], Tao Li[3], Ling-zhe Fang[3], Yubo Xing[2],* Jin-Cheng Li[1],*

[1]Faculty of Chemical Engineering, Yunnan Provincial Key Laboratory of Energy Saving in Phosphorus Chemical Engineering and New Phosphorus Materials, Kunming University of Science and Technology, Kunming 650500, China.

[2]Faculty of Metallurgical and Energy Engineering, National and Local Joint Engineering Research Center for Lithium-ion Batteries and Materials Preparation Technology, Key Laboratory of Advanced Battery Materials of Yunnan Province, Kunming University of Science and Technology, Kunming 650500, China.

[3]Department of Chemistry and Biochemistry Northern Illinois University DeKalb, IL 60115, USA.

E-mail: yuboxing@kust.edu.cn; jinchengli@kust.edu.cn

Experimental Section

1. Materials preparation

1.1. Materials

The pristine carbon nanotubes (CNTs) with average diameter of 20 nm were purchased from XIANFENG NANO. Nickel nitrate hexahydrate ($Ni(NO_3)_2 \cdot 6H_2O$, 98%) was purchased from Chongqing ChuanDong chemical engineering. Iron (III) nitrate nonahydrate ($Fe(NO_3)_3 \cdot 9H_2O$, 98%) was purchased from Damas-beta. Sodium hydroxide (NaOH) and sodium carbonate (Na_2CO_3) were purchased from Sigma Aldrich. Iron (II) phthalocyanine (FePc, 98%) was purchased from RHAWN. All reagents were used without further purification.

1.2. Preparation of FeNi-HO/CNT

1.0 g carbon nanotube (CNT) sample (purchased from Nanjing XFNANO Materials Tech Co., Ltd.) was suffered from oxidation treatment under a mixture solution (200 ml) of concentrated nitric acid and concentrated sulfuric acid with a volume ratio of 3:1 for 6 h to achieve oxidized CNT sample. Then, the oxidized CNT sample was dispersed in deionized water by ultrasound treatment for 4 h to achieve 0.1 mg ml^{-1} of CNT solution. Subsequently, 10 ml of Ni^{2+}/Fe^{3+} mixed solution (0.015 M nickel nitrate and 0.005 ferric nitrate) was added into 400 ml of the CNT solution under stirring, followed by treatment in oil bath at 80°C for 30 min. A mixed solution of 1 M sodium hydroxide and 0.01 M sodium carbonate was added in the above solution to adjust the pH value of ~10 to ensure the coprecipitation reaction. After the reaction for 24 h, FeNi hydroxide/oxyhydroxide particles anchored on CNT (FeNi-HO/CNT) was collected by centrifuging, washing and freeze-drying.

1.3. Preparation of FeNi/CNT

FeNi-HO/CNT was suffered from calcining process in a tube furnace under the argon atmosphere. A two-stage programmed heating process was carried out. First step was heating up to 500 ℃ from room temperature with a rate of 5 ℃ min^{-1}. Second step was kept at 500 ℃ for 2 h and then heating was stopped. After the tube furnace temperature cooled down, the FeNi/CNT sample, in which FeNi nanoparticles were inserted the wall of CNT due to carbothermic reaction, was obtained.

1.4. Preparation of FeNi/CNT-FePc

25 mg of iron phthalocyanine (FePc) was dissolved in 60ml of dimethylformamide through ultrasonic dispersion for 10 min. Then, 25 mg of FeNi/CNT was added in the FePc solution under ultrasonic treatment to ensure the coupling of FeNi/CNT and FePc. After coupling treatment for 1 h, the FeNi/CNT-FePc sample, in which FePc was anchored on the CNT wall, was achieved by filtering, washing and drying.

2. Material Characterization

The obtained materials were characterized by scanning electron microscopy (SEM, Nova NanoSEM 430, operated at 10 kV), transmission electron microscopy (Tecnai F20, 200 kV; Titan Cubed Themis G2, 300 kV), Raman spectroscopy (Jobin Yvon HR800), X-ray photoelectron spectroscopy (XPS, Escalab 250, Al Kα), Fourier transform infrared spectroscopy (FTIR, Bruker VERTEX 70 spectrometer), and X-ray diffraction (XRD, Rigaku Miniflex 600, 40 kV).

X-ray absorption spectroscopy measurement at Fe K-edge was performed at the

Advanced Photon Source on the bending-magnet beamline 9-BM-B with electron energy of 7 GeV and average current of 100 mA. The radiation was monochromatized by a Si (111) double-crystal monochromator. Harmomic rejection was accomplished with Harmonic rejection mirror. All spectra were collected in fluorescence mode by vortex four-element silicon drift detector. XAS data reduction and analysis were processed by Athena software.

3. Electrochemical Measurements

Electrochemical measurements were performed on an electrochemical analysis station (CHI 700 E, CH Instruments, China) using a standard three-electrode cell. A graphite rod and an Ag/AgCl electrode in a saturated KCl solution served as the counter electrode and reference electrode, respectively. All potential values refer to that of a reversible hydrogen electrode (RHE). To prepare the working electrode, 5.0 mg of each catalyst was ultrasonically dispersed in ethanol containing 0.05 wt.% Nafion (1.0 ml) to form a concentration of 5.0 mg ml^{-1} catalyst ink. The catalyst ink was then coated on the surface of the glassy carbon disk for the RRDE and RDE tests. The noble-metal-free catalyst loading was 0.5 mg cm^{-2}. Commercial Pt/C (20 wt.%, Alfa Aesar) and Ir/C (20 wt.% of Ir, Premetek Co.) catalysts with a standard loading of 0.1 mg cm^{-2} were respectively used as ORR and OER reference samples. The linear scan voltammogram (LSV) curves in this work were corrected with *iR* compensation.

For the RRDE tests, the polarization curves were collected at disk rotation rates of 1600 rpm. The scan rate was 5 mV s^{-1} and the potential of ring was set at 0.3 V (vs. Ag/AgCl). The collecting efficiency of the RRDE (N) was 0.37. The peroxide yield

(HO_2^-%) and the electron transfer number (n) was calculated as follows:

$$HO_2{}^-\% = 200 \times \frac{I_r/N}{I_d + I_r/N}$$

$$n = 4 \times \frac{I_d}{I_d + I_r/N}$$

where I_d is the disk current and I_r is the ring current. The ORR durability was evaluated by testing the LSV of FeNi/CNT-FePc modified electrode at 1600 rpm before and after 5000 continuous cyclic voltammetry (CV) potential cycles.

The RDE polarization curves for the OER were collected in 0.1 M KOH solution at a disk rotation rate of 1600 rpm. The scan rate was 5 mV s^{-1}. The OER durability was evaluated by testing the LSV of FeNi/CNT-FePc modified electrode at 1600 rpm before and after 5000 continuous CV potential cycles.

4. ZAB Tests

ZABs were assembled in homemade cells. Catalyst ink was loaded on a porous carbon paper as the air electrode. The catalyst loading was 0.8 mg cm^{-2}. A Zn plate was used as the anode. A 6 M KOH aqueous solution with 0.2 M zinc acetate was used as the electrolyte. Polarization curve measurements of ZABs were performed on an electrochemical analysis station (CHI 700E, CH Instruments, China). Galvanostatic charge-discharge cycling measurements of ZABs were carried out on battery testing system (CT-4008, NEWARE, China).

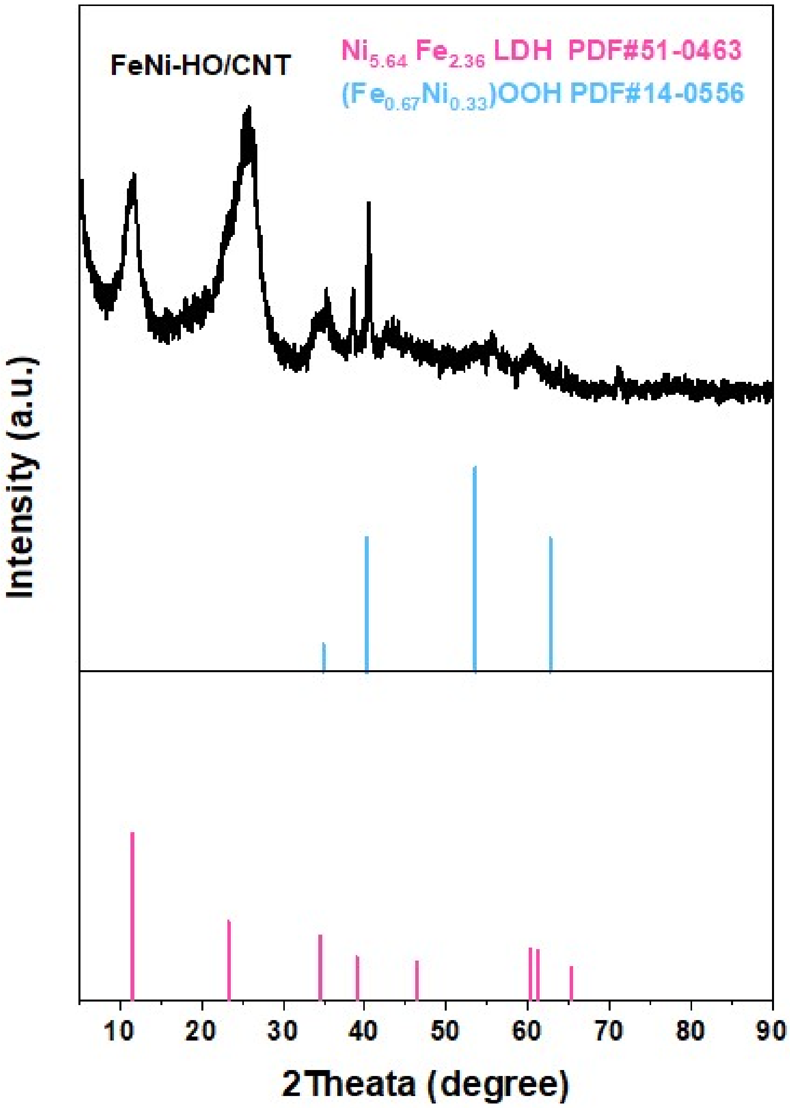

Figure S1. XRD pattern of FeNi-HO/CNT.

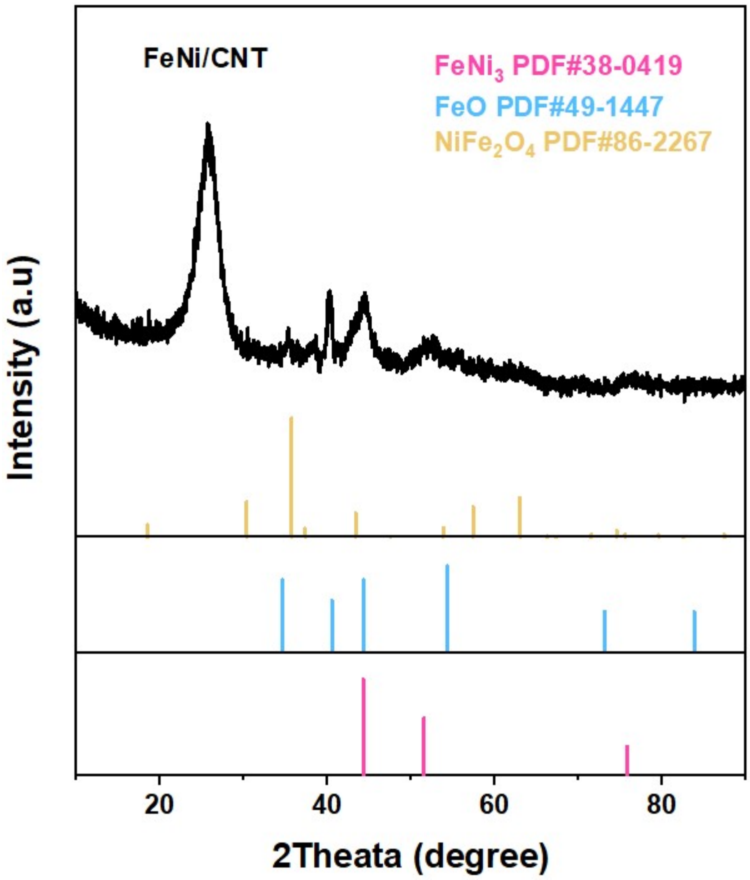

Figure S2. XRD pattern of FeNi/CNT.

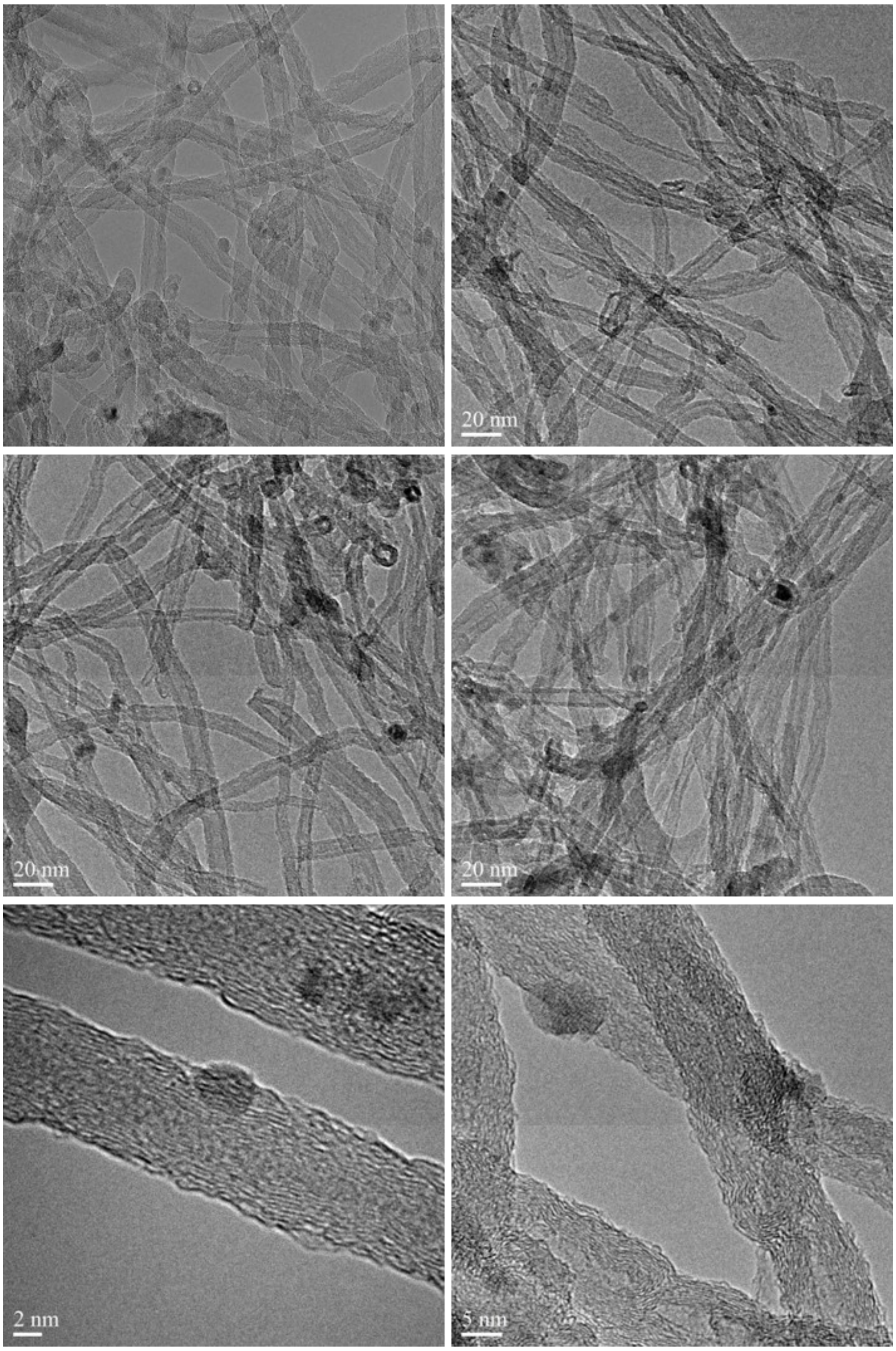

Figure S3. TEM images of FeNi/CNT-FePc.

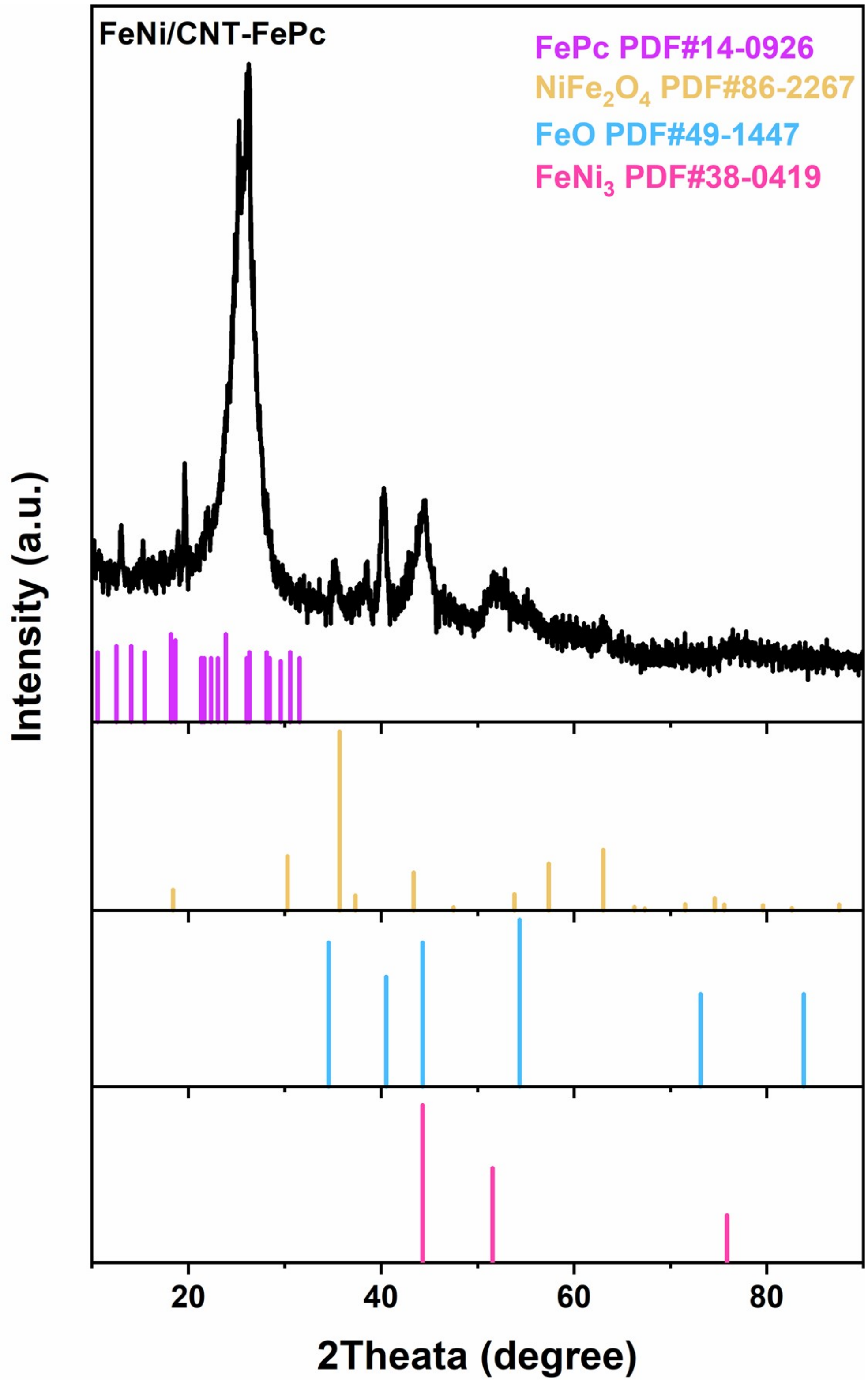

Figure S4. XRD pattern of FeNi/CNT-FePc.

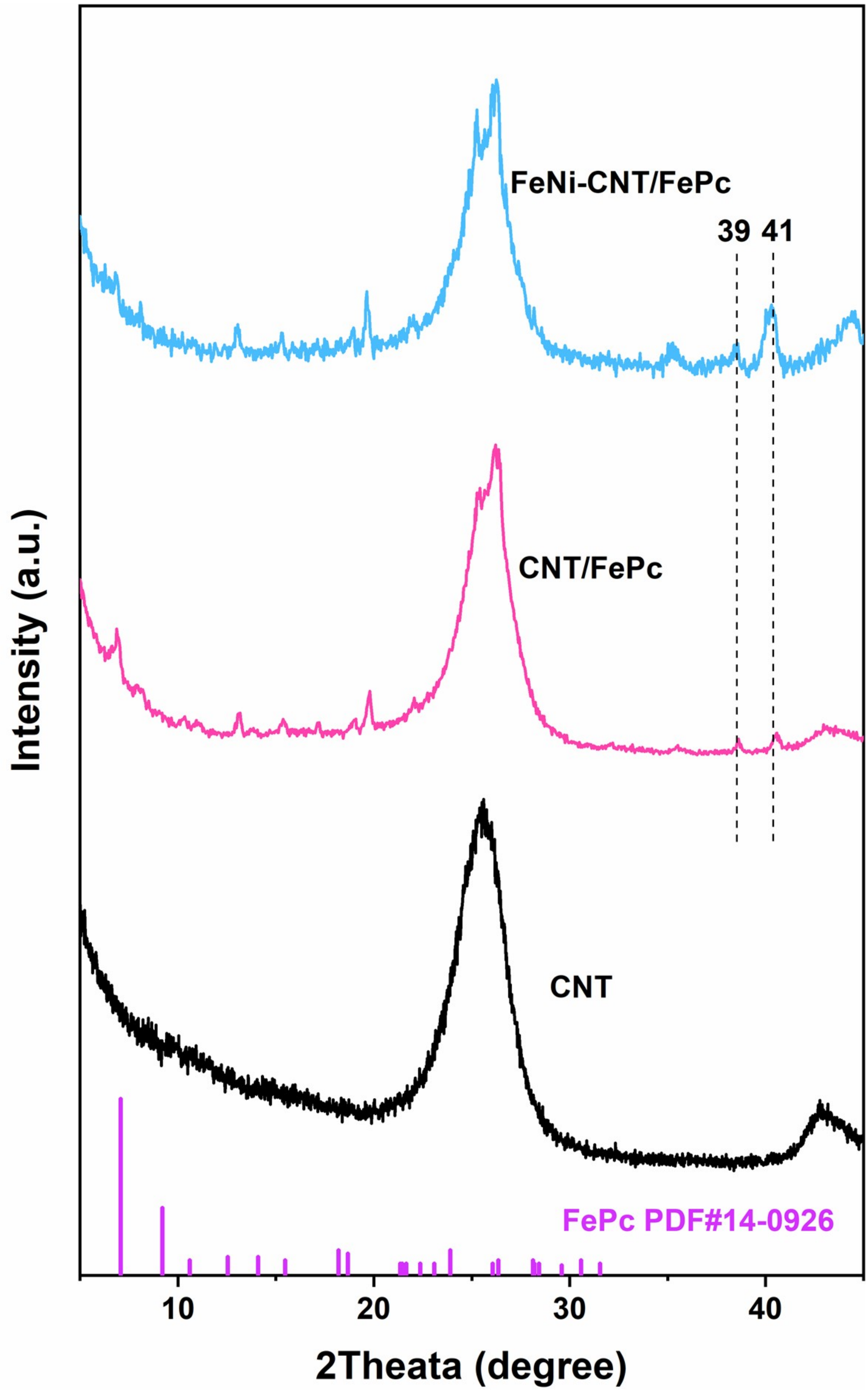

Figure S5. XRD patterns of FeNi/CNT-FePc and reference samples.

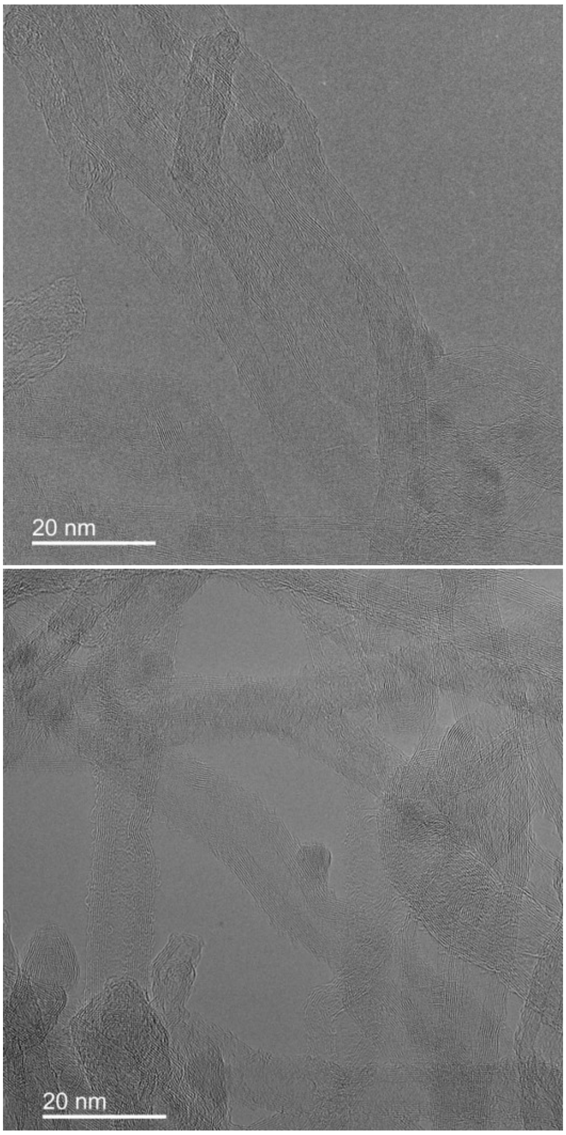

Figure S6. Bright-field STEM images of FeNi/CNT-FePc.

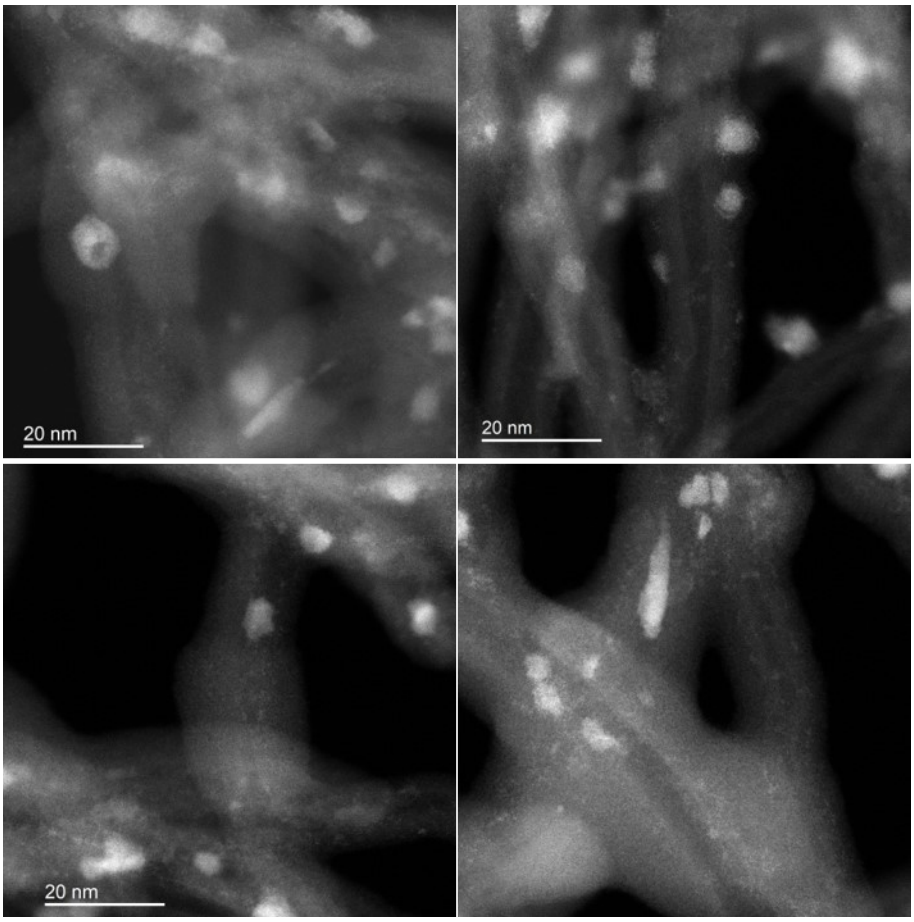

Figure S7. HAADF-STEM images of FeNi/CNT-FePc.

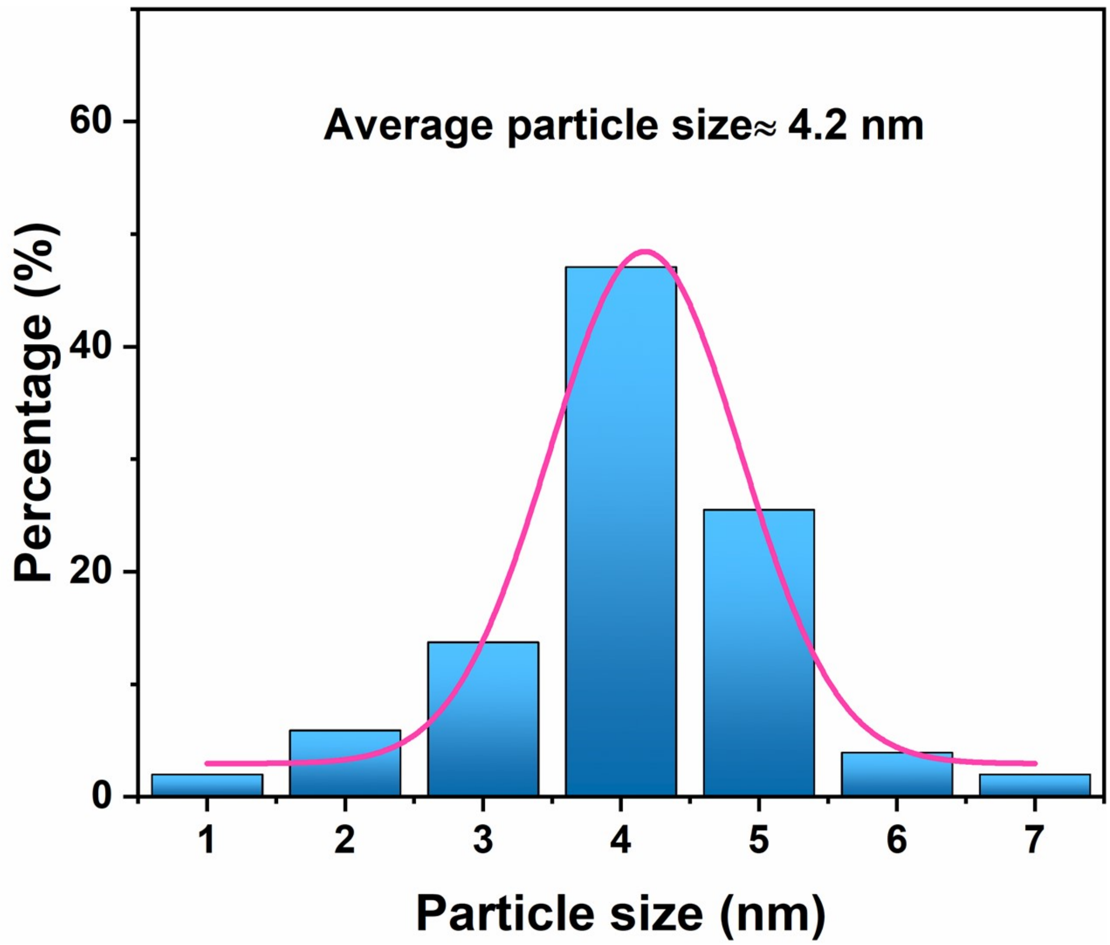

Figure S8. Metal particle size distribution in FeNi/CNT-FePc.

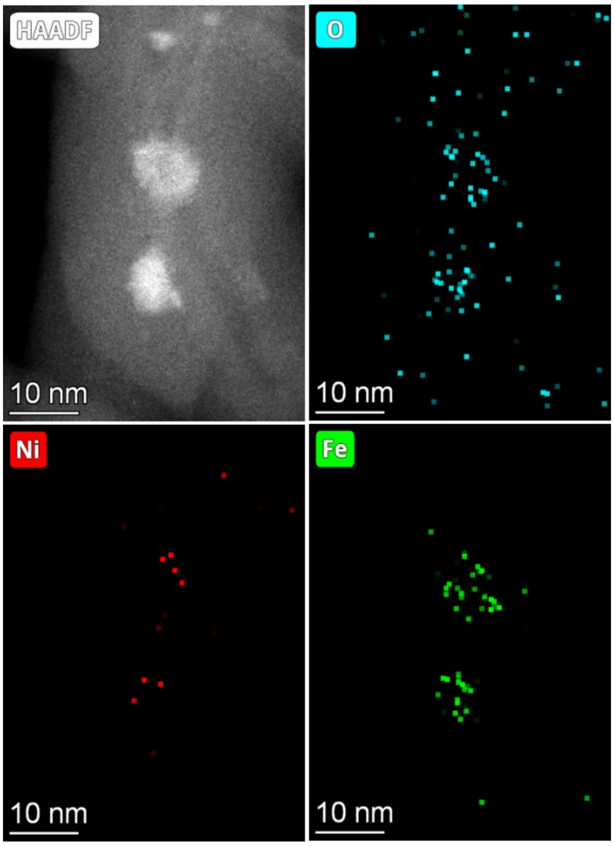

Figure S9. HAADF-STEM image of FeNi/CNT-FePc and the corresponding EDS mapping.

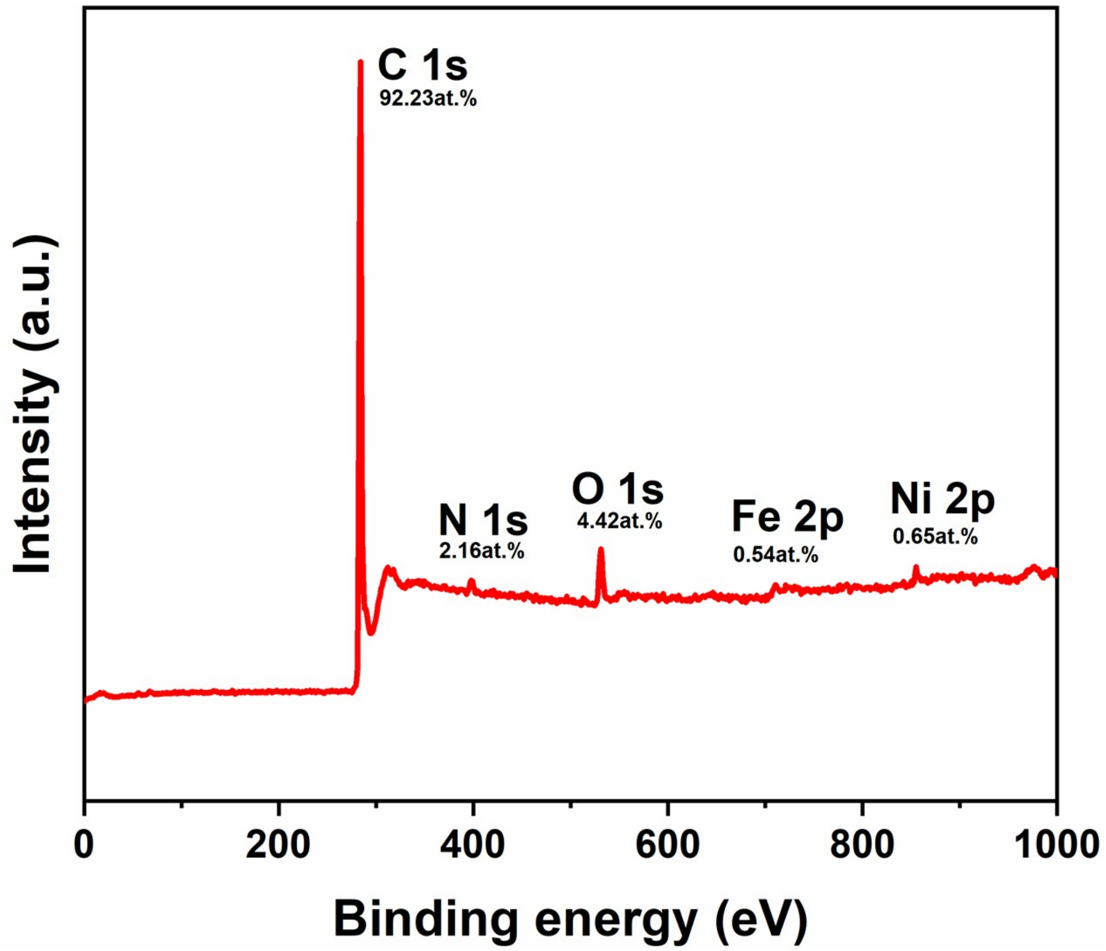

Figure S10. XPS spectrum showing the presence of C, N, O, Fe and Ni and their contents in FeNi/CNT-FePc.

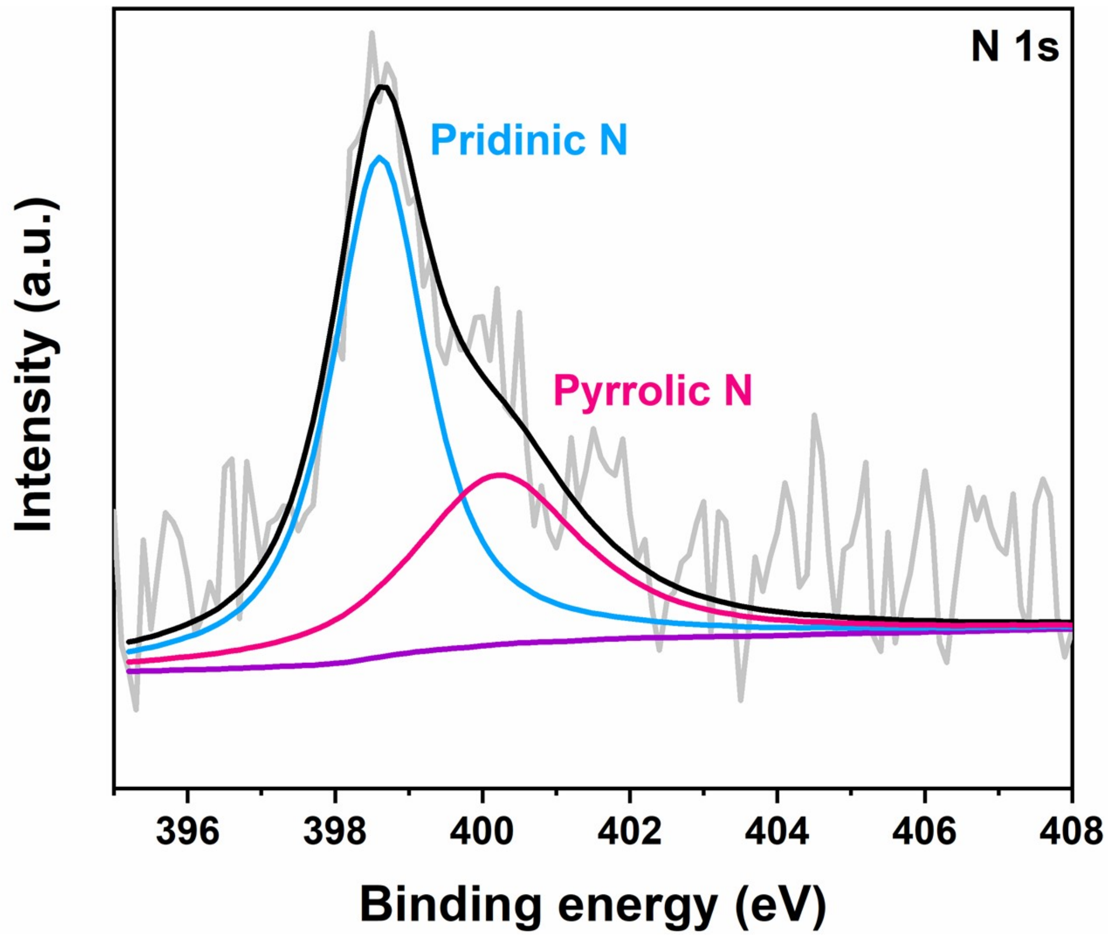

Figure S11. N 1s XPS spectrum of FeNi/CNT-FePc.

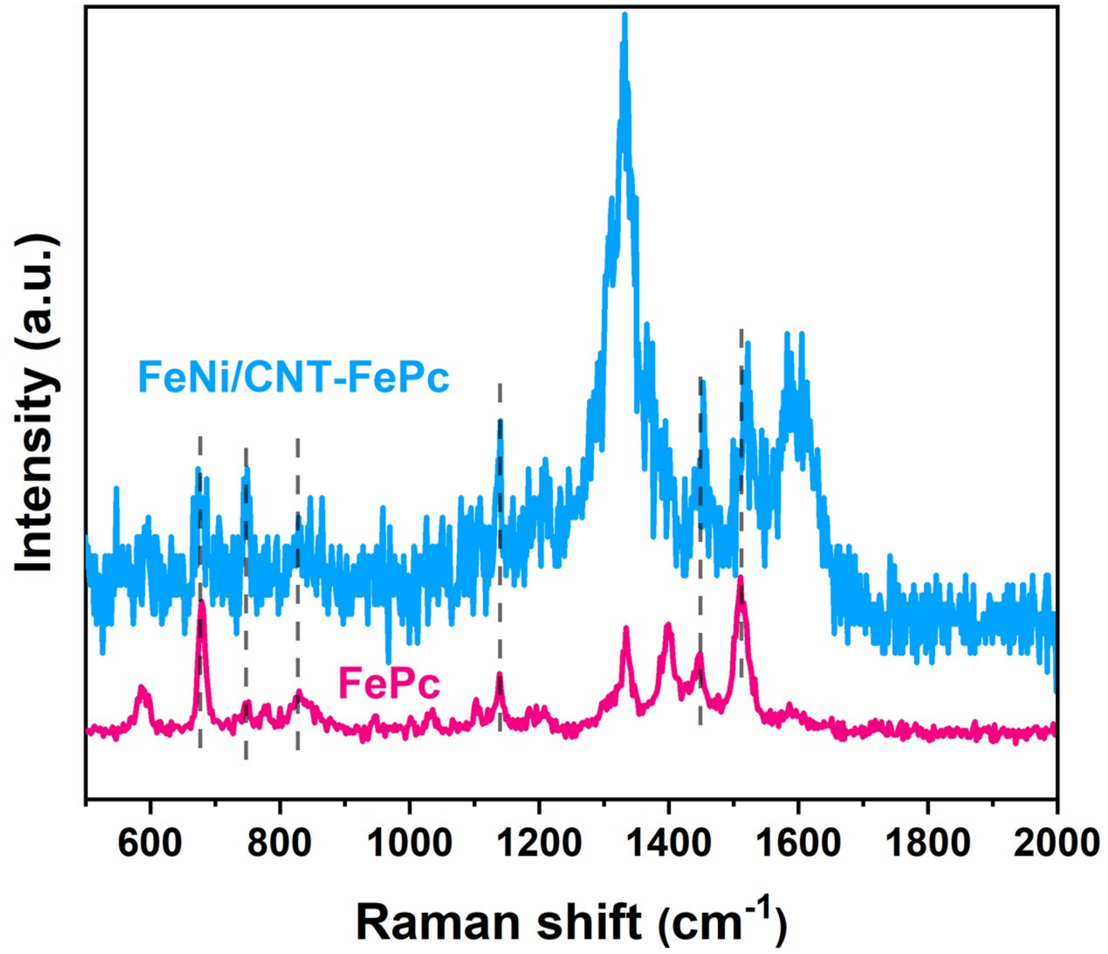

Figure S12. Raman spectra of FeNi/CNT-FePc and FePc.

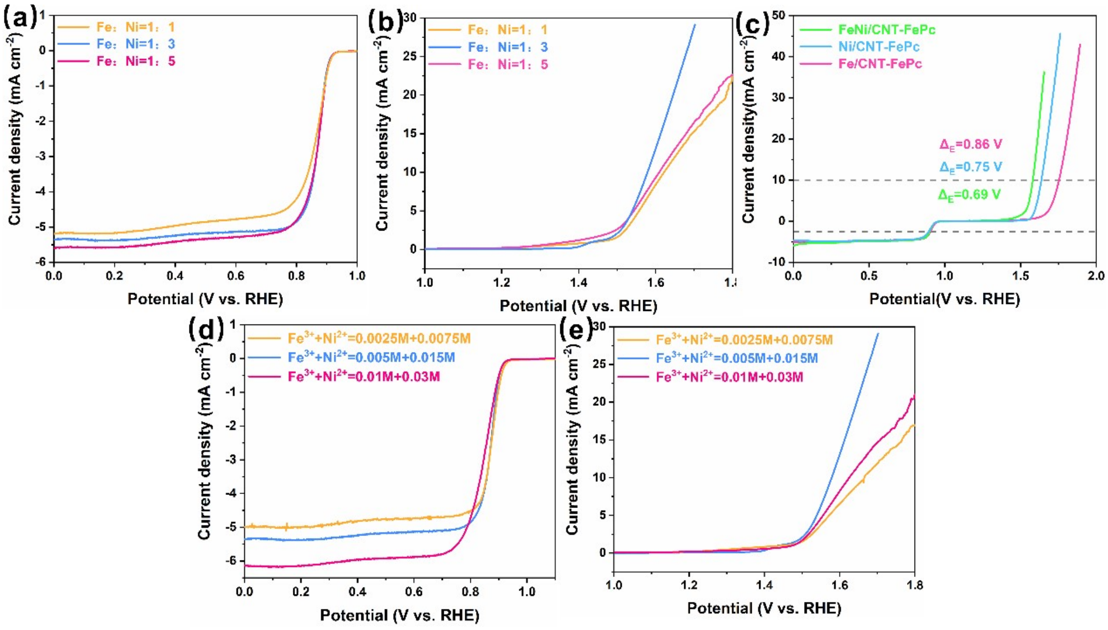

Figure S13. Oxygen electrocatalytic reaction performances of FeNi/CNT-FePc, Fe/CNT-FePc and Ni/CNT-FePc.

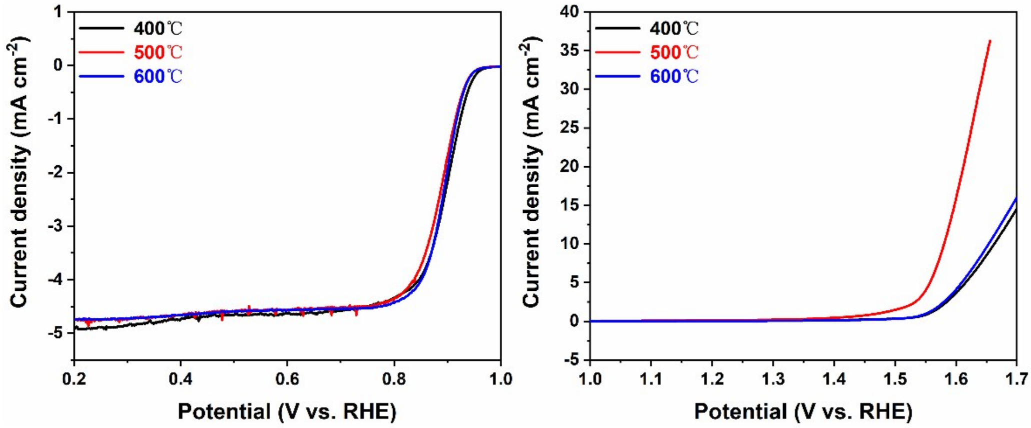

Figure S14. Performance optimization by modulating carbothermic reaction temperatures.

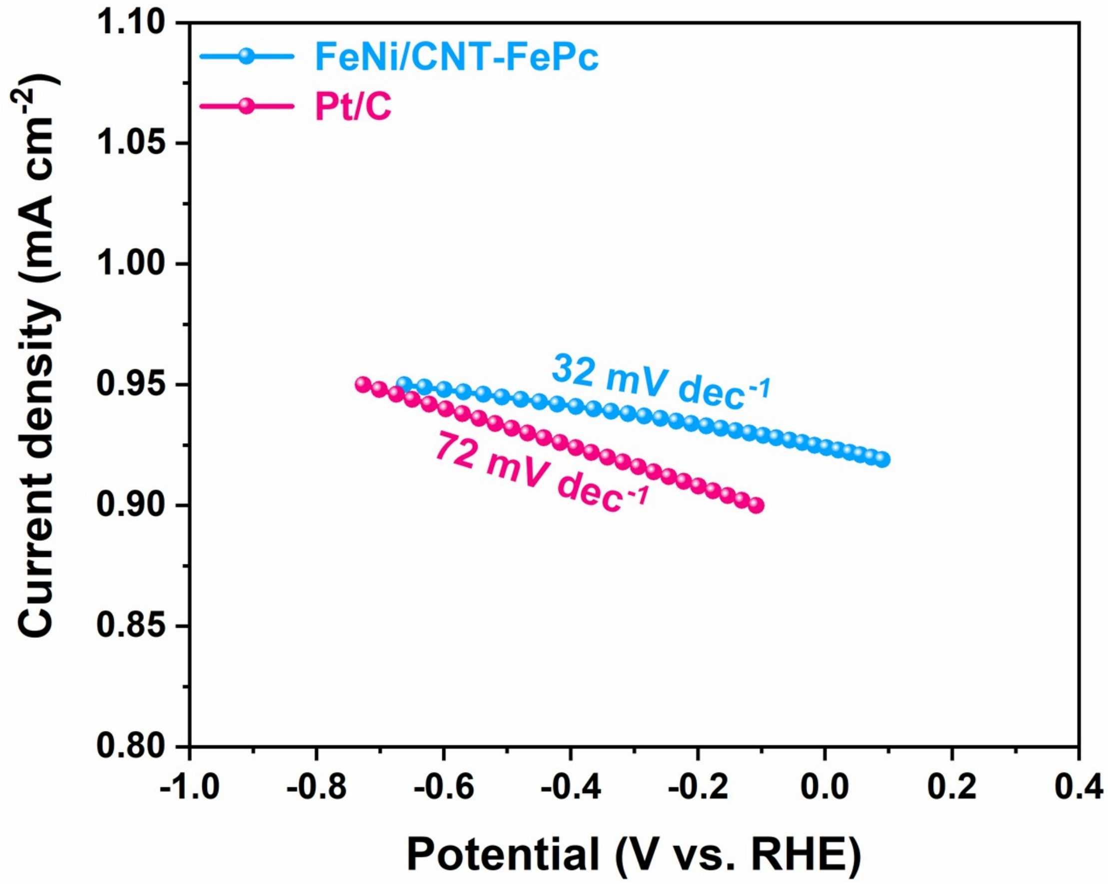

Figure S15. Tafel plots of FeNi/CNT-FePc and Pt/C for ORR.

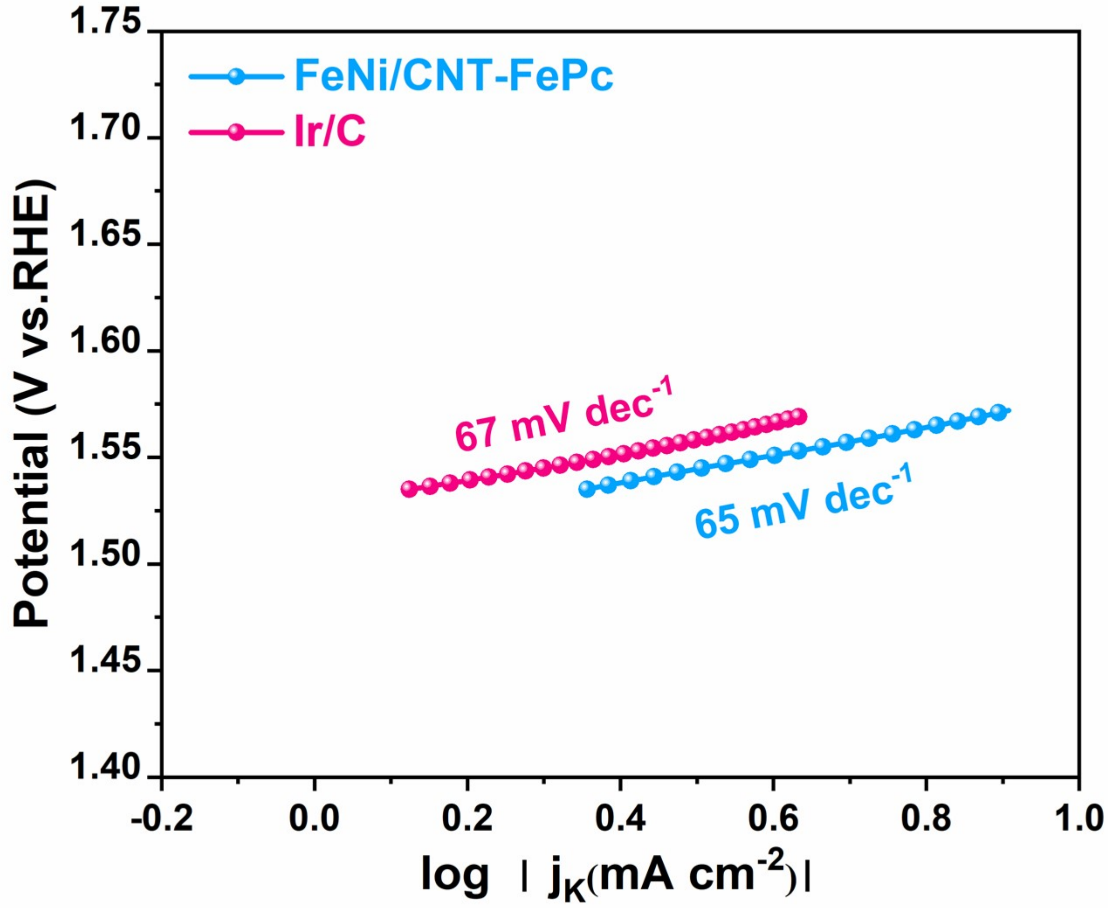

Figure S16. Tafel plots of FeNi/CNT-FePc and Ir/C for OER.

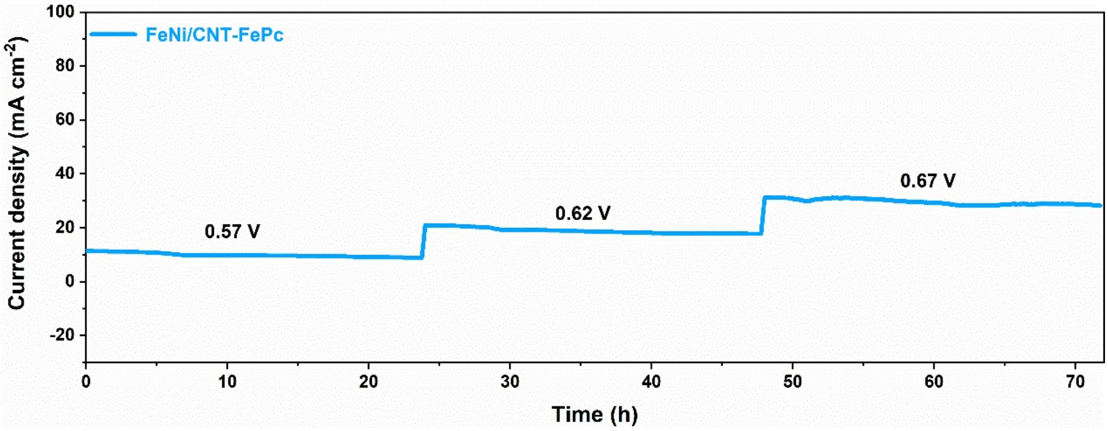

Figure S17. i-t curve of FeNi/CNT-FePc for OER.

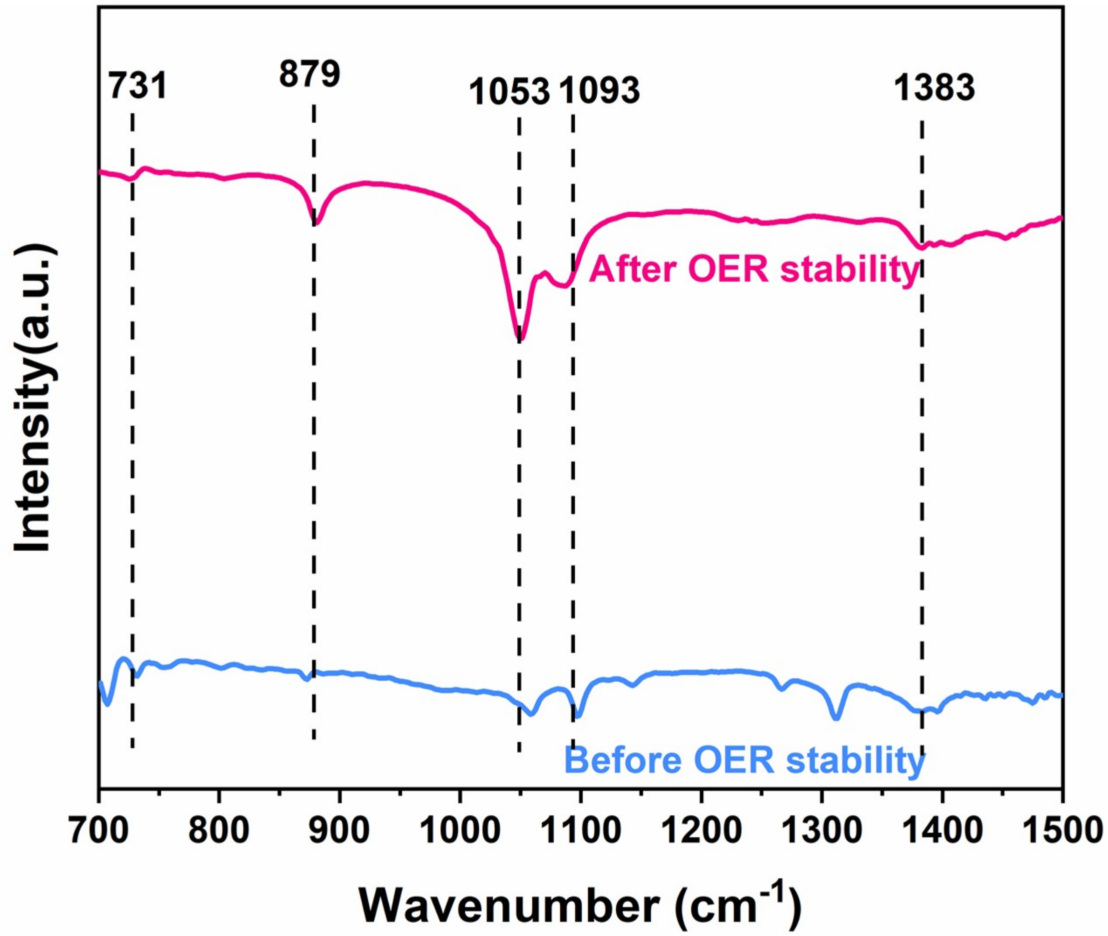

Figure S18. FTIR spectra of FeNi/CNT-FePc before and after OER stability.

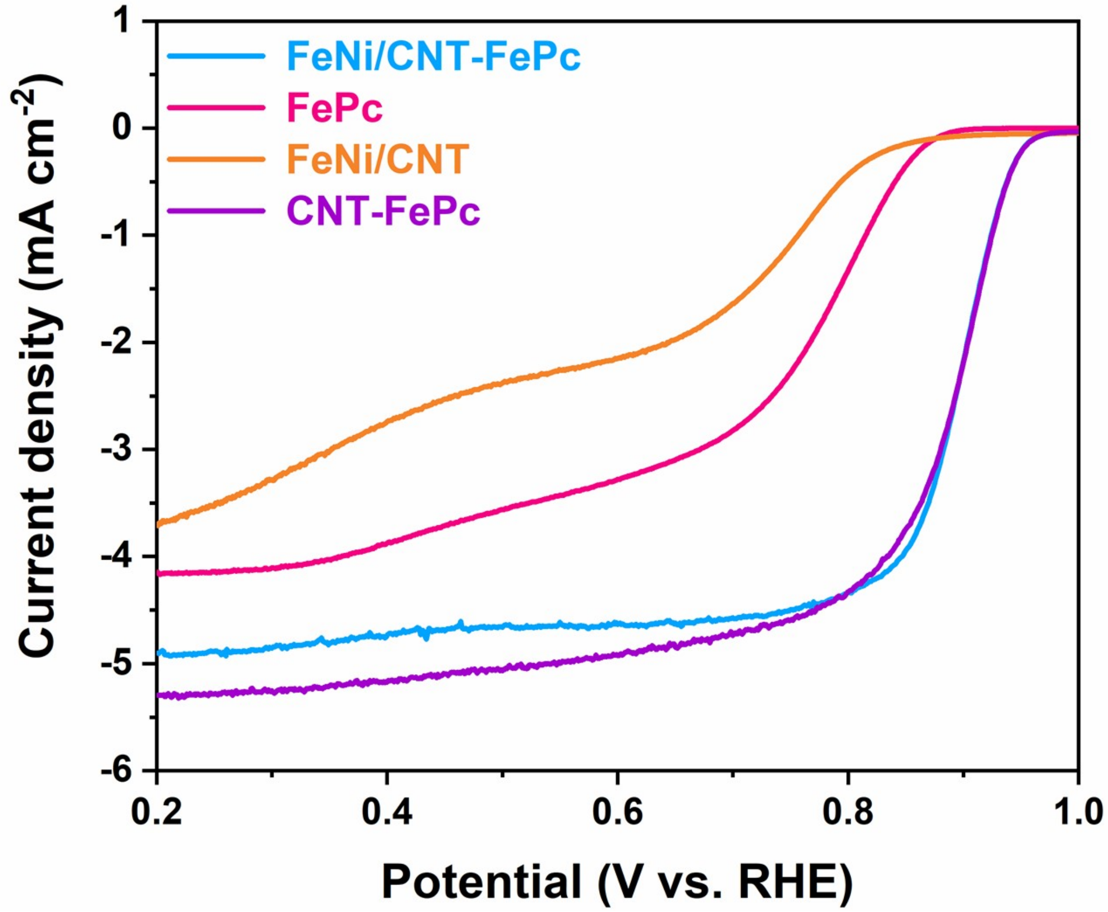

Figure S19. ORR polarization curves of FeNi/CNT-FePc, FeNi/CNT, FePc and CNT-FePc.

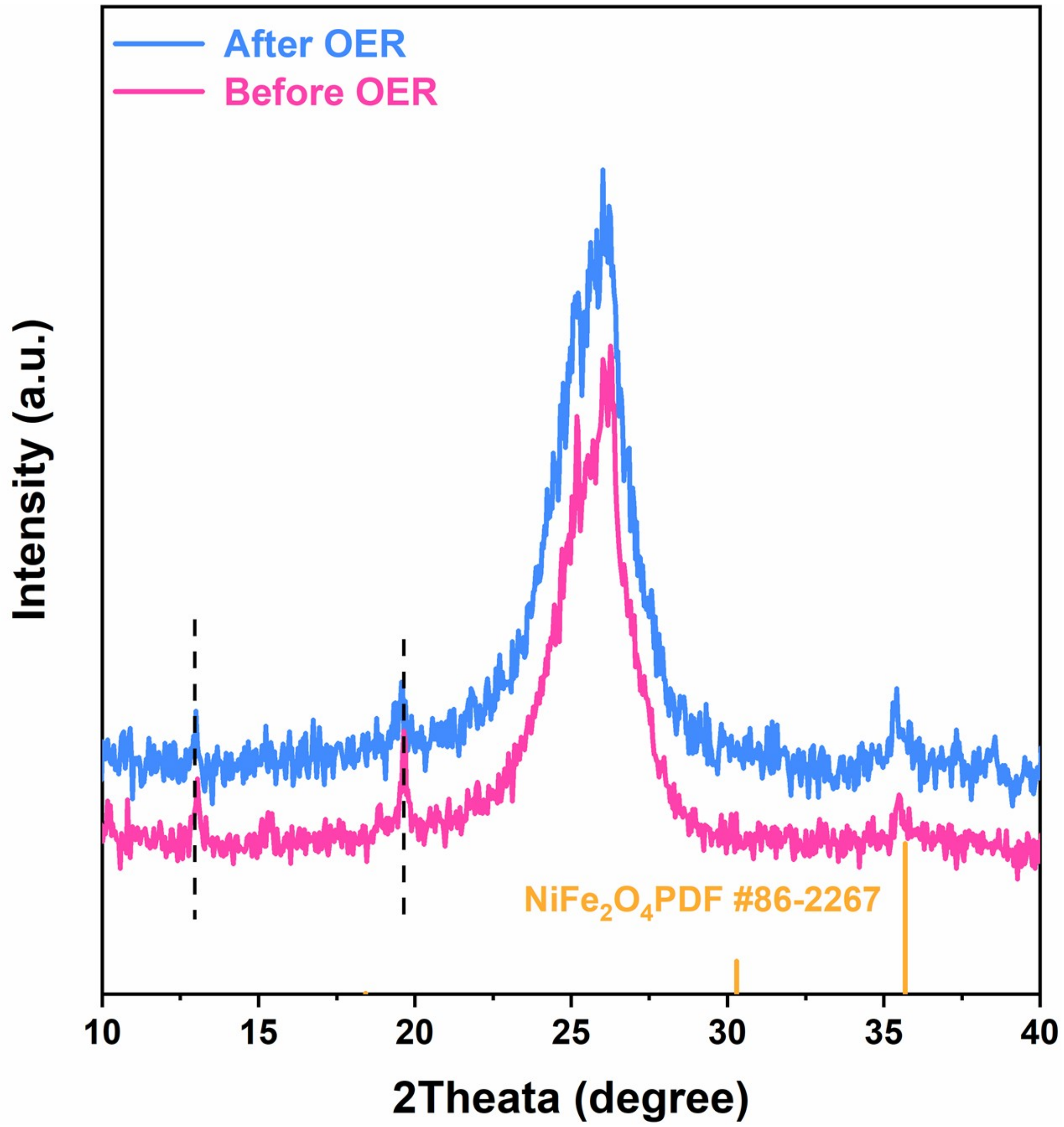

Figure S20. XRD patterns of FeNi/CNT-FePc before and after the OER tests.

Figure S21. Open circuit voltage of liquid-state ZAB assembled by using Pt/C+Ir/C as the cathodic electrocatalyst.

Figure S22. Open circuit voltage of liquid-state ZAB assembled by using FeNi/CNT-FePc as the cathodic electrocatalyst.

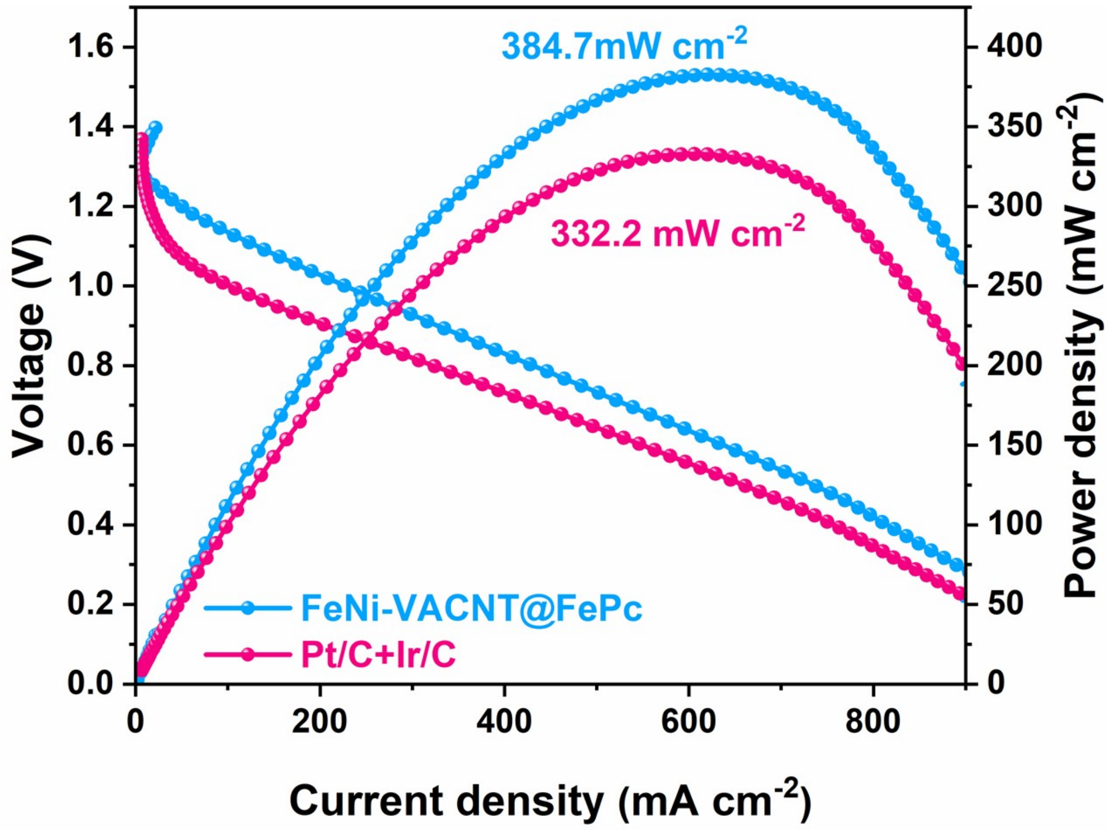

Figure S23. Oxygen atmosphere power density curves of liquid-state ZABs based on FeNi/CNT-FePc and Pt/C+Ir/C.

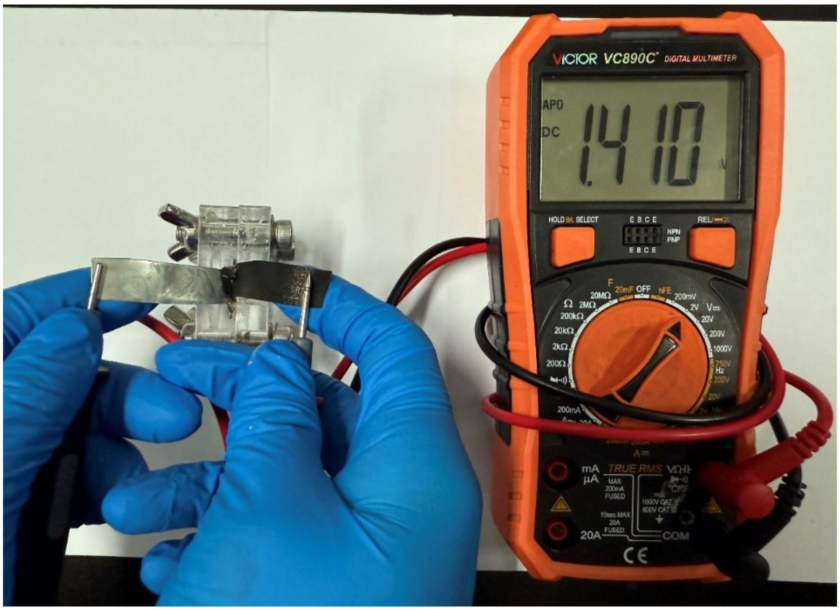

Figure S24. Open circuit voltage of solid-state ZAB assembled by using FeNi/CNT-FePc as the cathodic electrocatalyst.

Figure S25. Open circuit voltage of solid-state ZAB assembled by using Pt/C+Ir/C as the cathodic electrocatalyst.

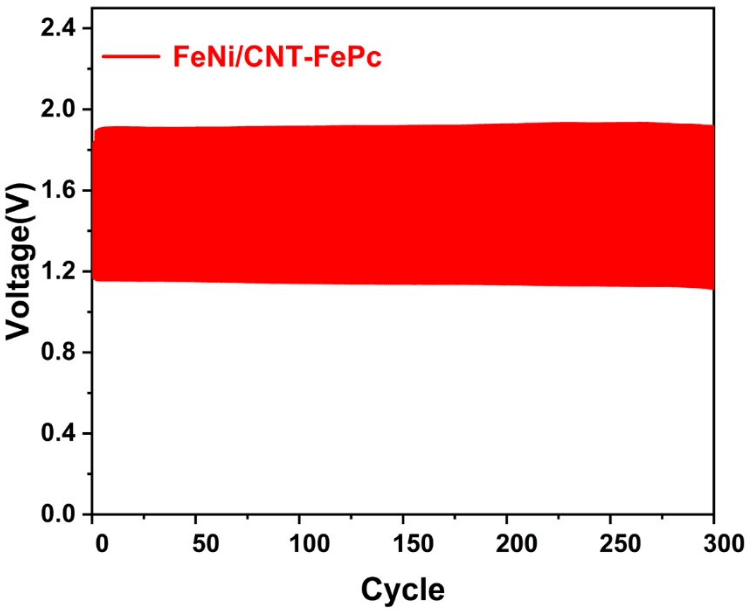

Figure S26. Galvanostatic charge–discharge cycling curve of the FeNi/CNT-FePc-based solid-state ZAB at 2 mA cm^{-2}.

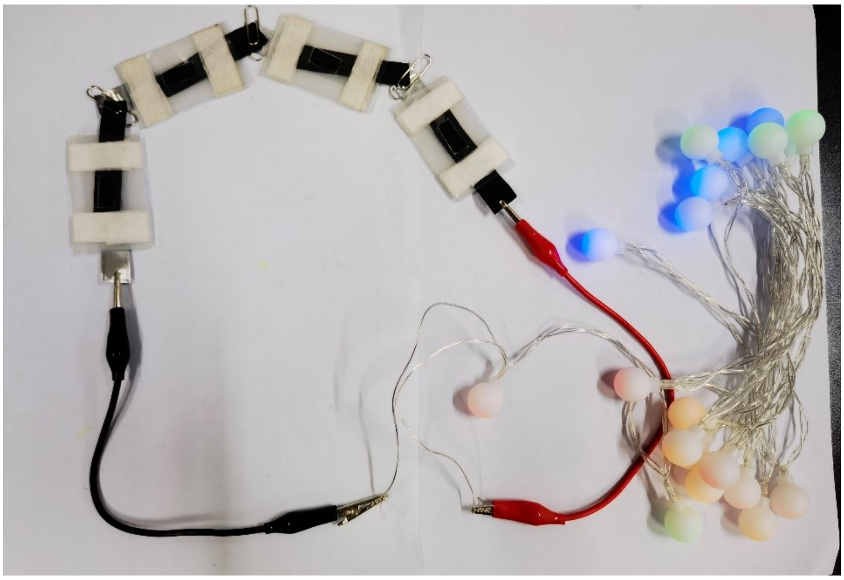

Figure S27. Photograph showing a string of colored lights brighten by FeNi/CNT-FePc-based solid-state ZABs.

Table S1. An oxygen electrocatalytic performance comparison of carbon-based noble-metal-free catalysts

Electrocatalysts	**Potential difference (V)**	**References**
A-MnO_2/NSPC-2	0.64	*Adv. Mater. 2024, 36, 2312868*
CoFe/CoFeP@NPC	0.663	*Nano Energy, 2024,110497*
Ni,Fe-DSAs/NCs	0.717	*ACS Nano, 2023, 17, 8622-8633*
NiFe-LDH/Fe1-N-C	0.65	*Adv. Energy Mater., 2023, 13, 2203609*
Co-CoN_4@NCNs	0.71	*Adv. Funct. Mater. 2022,32,2207331*
Co_p@CoNC	0.68	*Energy Storage Mater., 2022, 46, 553-562*
CoFe/S-N-C	0.733	*Chem. Eng. J., 2022,429, 132174.*
FeNi/CNT-FePc	**0.66**	***This Work***

Table S2. A liquid-state ZAB performance comparison of advanced ZABs based noble-metal-free electrocatalysts.

Electrocatalyst	**Peak power density （mW cm^{-2}）**	**References**
FeCo-NPC	165	*Adv. Mater. 2023, 2306047.*
Se doped MOF CoS$_2$ HSs@CC	156.24	*Appl. Catal. B 2023, 330. 122523*
Ni$_{SA}$Fe$_{SA}$-Ni@F$_{eNPs}$/CNTs-NGNS	163.04	*Chem. Eng. J. 2022, 440,135781*
FeCo/Se-CNT	173.4	*Nano Lett. 2021, 21, 2255-2264*
D–Co@NC	115.4	*Chem. Eng. J. 2022, 431,133734*
Co–MOF–800	144	*Energy Chem.2021, 56,290-298*
CoFeN-NCNTs//CCM	145	*Adv. Funct. Mater., 2022, 32, 2107608*
FeMn-DSAC	184	*Angew. Chem. Int. Ed. 2022, 61, e202115219.*
FeNi/CNT-FePc	**208.5**	***This Work***